Using Amphiphilic Nanostructures To Enable Long-Range Ensemble Coalescence and Surface Rejuvenation in Dropwise Condensation

David M. Anderson,[†] Maneesh K. Gupta,[‡] Andrey A. Voevodin,[§] Chad N. Hunter,[§] Shawn A. Putnam,[§,∥] Vladimir V. Tsukruk,[‡] and Andrei G. Fedorov[†,⊥,*]

[†]G. W. Woodruff School of Mechanical Engineering and [‡]School of Materials Science and Engineering, Georgia Institute of Technology, Atlanta, Georgia 30332, United States, [§]Air Force Research Laboratory, Thermal Sciences and Materials Branch, Wright-Patterson AFB, Ohio 45433, United States, [∥]Universal Technology Corporation, Dayton, OH 45432, United States, and [⊥]Parker H. Petit Institute of Bioengineering and Bioscience, Georgia Institute of Technology, Atlanta, Georgia 30332, United States

ABSTRACT

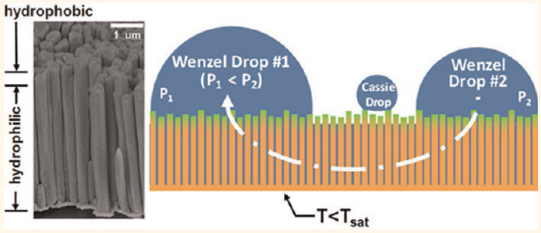

Controlling coalescence events in a heterogeneous ensemble of condensing droplets on a surface is an outstanding fundamental challenge in surface and interfacial sciences, with a broad practical importance in applications ranging from thermal management of high-performance electronic devices to moisture management in high-humidity environments. Nature-inspired superhydrophobic surfaces have been actively explored to enhance heat and mass transfer rates by achieving favorable dynamics during dropwise condensation; however, the effectiveness of such chemically homogeneous surfaces has been limited because condensing droplets tend to form as pinned Wenzel drops rather than mobile Cassie ones. Here, we introduce an amphiphilic nanostructured surface, consisting of a hydrophilic base with hydrophobic tips, which promotes the periodic regeneration of nucleation sites for small droplets, thus rendering the surface self-rejuvenating. This unique amphiphilic nanointerface generates an arrangement of condensed Wenzel droplets that are fluidically linked by a wetted sublayer, promoting previously unobserved coalescence events where numerous droplets simultaneously merge, without direct contact. Such ensemble coalescences rapidly create fresh nucleation sites, thereby shifting the overall population toward smaller droplets and enhancing the rates of mass and heat transfer during condensation.

KEYWORDS: amphiphilic nanostructures · environmental scanning electron microscopy · nanoscale water condensation · droplet coalescence dynamics

Though wettability has long been understood to depend on surface chemistry and morphology,[1] intriguing opportunities to control nanostructure and create surface energy gradients with novel nanofabrication techniques have recently generated a surge of research interest in this field.[2−4] Such surfaces elucidate previously unknown modes of droplet dynamics during condensation and challenge the current understanding of physical mechanisms at multiple length scales[5] that underlie different stages of the process, especially relevant to collective droplet dynamics during growth and coalescence.[6] These new insights can be harnessed to design "smart" nanostructured interfaces which can intrinsically (*i.e.*, without external stimuli) control the dynamics of droplet nucleation, growth, and coalescence events to maximize heat and mass transfer rates. Such advances are critical for emerging micro/nanotechnologies, including high-performance microprocessors, high-energy density batteries, and optoelectronic devices, which are becoming thermally limited and require major advances in our ability to control phase-change phenomena on the nanoscale.

The manner in which condensed liquid interacts with the underlying substrate has a dramatic effect on the achievable rate of heat and mass transfer on a surface. Dropwise condensation, in which the surface is not uniformly wetted, provides heat and mass transfer coefficients over an order of magnitude higher than its filmwise counterpart.[7−9] Droplets are continually swept off a surface by gravity or vapor shear to allow repetition of the droplet nucleation and growth process, which is most efficient for moisture/heat management,[10,11] in contrast to filmwise condensation where heat and mass transfer is restricted by a growing condensed liquid layer with limited thermal conductivity. Droplets typically leave the surface by a rolling mechanism; therefore, contact line pinning and contact angle

* Address correspondence to AGF@gatech.edu.

Received for review January 13, 2012 and accepted March 28, 2012.

Published online March 28, 2012
10.1021/nn300183d

hysteresis must be minimized to promote easy removal. So-called "Cassie" droplets, resting on a heterogeneous interface consisting of air and the tips of roughness features, are substantially more mobile than "Wenzel" droplets, which penetrate the roughness features to form a homogeneous solid–liquid interface and thus suffer from contact line pinning.[12,13] Surfaces which wet with mobile droplets exhibiting minimal contact angle hysteresis are termed superhydrophobic, and the extensive body of dropwise condensation research has focused on this type of surface and the associated rolling mechanism.[14–20] A widely recognized challenge with superhydrophobic surfaces, as observed in nature on the lotus leaf[21] and on synthetic surfaces,[22,23] is that they are often rendered ineffective during condensation because the Wenzel state is typically at a lower interfacial free energy than the Cassie state.[24–26] As a result, metastable Cassie droplets may initially form on the surface, but eventually droplets condensed from the surrounding vapor phase will revert to the pinned Wenzel state, as opposed to deposited droplets which assume the Cassie state and roll easily off the surface. The only notable exceptions are surfaces which require complex, two-tier roughness.[15–17]

Here, we introduce an amphiphilic surface consisting of densely packed nanowires made of hydrophilic base material with hydrophobic tips which demonstrate the ability to produce long-range, noncontact coalescence events within a heterogeneously sized droplet ensemble to periodically regenerate nucleation sites, without requiring condensed droplets to remain stable in the mobile Cassie state! To demonstrate this intriguing phenomenon, we performed complementary optical visualization with visible light and environmental scanning electron microscopy (ESEM) imaging of droplet condensation on a subcooled amphiphilic nanostructure and report a mode of coalescence involving numerous droplets simultaneously merging with no direct contact above the surface. We propose a new mechanism of coalescence, involving Laplace pressure imbalance between adjacent fluidically linked droplets, for these events which rapidly open up fresh nucleation sites thus rejuvenating the surface and generating a favorable distribution of smaller droplets attractive to heat/mass transfer.

RESULTS AND DISCUSSION

Amphiphilic Nanostructured Surface. The nanowire array, shown in Figure 1, consists of 200 nm diameter hydrophilic gold wires that are coated from the top with a hydrophobic fluoropolymer using plasma-enhanced chemical vapor deposition (PECVD).[27] Because PECVD is a directional process, the fluoropolymer only coats the tips of the nanowires, creating a surface energy gradient of low-energy hydrophobic coating on the nanowire tips and native hydrophilic gold at the base. This arrangement of vertical surface energy gradient with low energy at the roughness tips with high energy at the base on a condensing surface is a departure from most efforts to design robust dropwise condensing surfaces, which utilize uniform hydrophobic coating methods. Studies that have varied the surface energy have done so with a radial gradient[28] or hydrophilic tips on hydrophobic base features.[18]

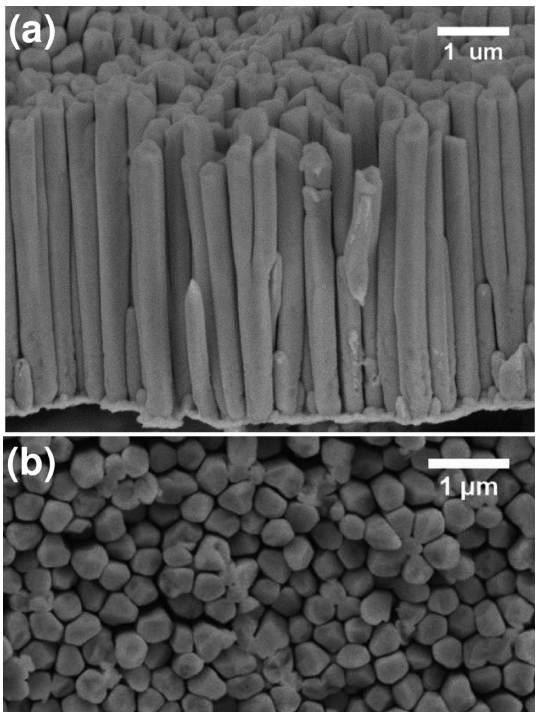

Figure 1. (a) Side and (b) overhead SEM micrographs showing nanostructured surface morphology.

The array is closely packed with less than 25 nm separating adjacent wires and an estimated packing fraction of 85%. The wires are also not uniform in height, creating a secondary roughness scale which allows droplets that do rest on its roughness features to only contact the tallest asperities and display a high contact angle by minimizing the amount of solid–liquid contact area. This secondary roughness scale is critical to the surface's condensation performance, as will be discussed later. The depth of penetration of the hydrophobic fluoropolymer coating is roughly 10% of the total wire length, as determined by ESEM visualization of the wetting of the hydrophilic base of the wires when the surface is cooled below the vapor saturation temperature by a Peltier cooler (web enhanced object S1).

Droplet Size Distribution during Condensation. The temporal evolution of the condensed droplet size distribution on a subcooled amphiphilic nanostructured surface is compared to that of a smooth silicon surface with hydrophobic coating. Optical visualization is used, rather than ESEM, for this comparison to obtain a larger field of view. Ambient temperature is held within ±0.5 °C and relative humidity within ±2.5%, and to ensure consistent

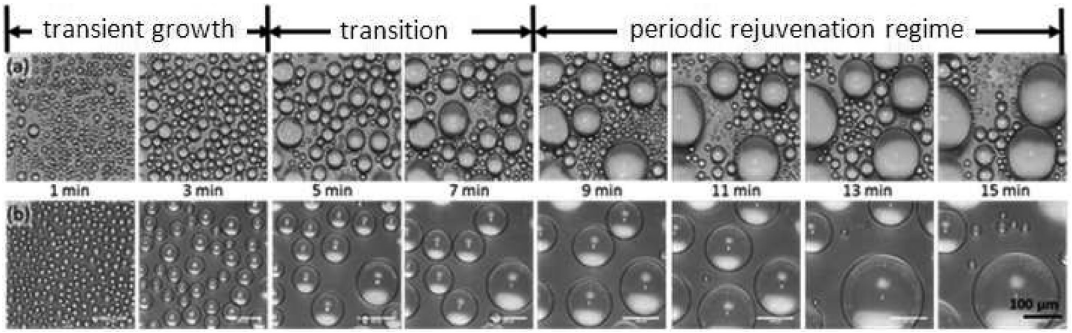

Figure 2. Temporal evolution of droplet size distribution during condensation on (a) amphiphilic nanostructured and (b) smooth hydrophobic surface.

subcooling between tests, DC power to a Peltier stage beneath the sample is controlled manually to cool the surface 4 °C below saturation temperature for the corresponding ambient conditions.

Representative images at various times past the onset of condensation are shown in Figure 2. During the initial transient growth, condensation appears similar on both the smooth hydrophobic and the amphiphilic nanostructured surfaces. After the third minute of condensation, different size droplets begin to form on the amphiphilic surface and coalescences simultaneously involving many droplets which are not in direct contact above the surface are observed. These unique coalescence events are most vividly observed in web enhanced object S2. As new droplets nucleate in the space cleared behind coalesced droplets, the process repeats itself in a periodic manner. In contrast, the droplets on the smooth hydrophobic surface mostly grow through further condensation, with coalescences only occurring in a traditional manner by adjacent droplets physically growing into one another.[29] As a result, during 15 min of condensation, the mean droplet size on the amphiphilic surface only reaches approximately 20 μm, while for the smooth hydrophobic surface, it continues to grow up above 100 μm.

The histograms in Figure 3 provide statistical information on the periodic nature of condensation on the amphiphilic surface by looking at evolution of the droplet distribution for two consecutive cycles in the periodic rejuvenation regime (see also web enhanced object S3). The first stage of this periodic behavior, a large spike in small droplets, occurs immediately following a major coalescence event as new droplets nucleate in the space left open behind the smaller droplets. This initial stage can be seen in the droplet distribution at 8 and 11 min past the onset of condensation. In the next stage, visible respectively at 9 and 12 min, the tall peak of smaller droplets in the distribution begins to flatten out and shift to the right (*i.e.*, toward few but larger droplets), as the smaller droplets coalesce with their nearest neighbors. In this second stage only 2−3 droplets coalesce at once in the traditional direct-contact induced manner, as indicated by the fact that the overall droplet count still remains relatively high. Lastly, long-range multidroplet collective coalescence events take place during the third stage, causing the droplet distributions at 10 and 13 min to flatten out with significant reduction in the small droplet count, thus creating fresh nucleation sites. The surface is able to "self-rejuvenate" in this manner, and because prior studies have shown that droplets with diameters less than 10 μm contribute the most to heat transfer during dropwise condensation,[10] this behavior is expected to enhance heat transfer by continually nucleating new micrometer-sized droplets.

Proposed Mechanism of Droplet Growth and Coalescence. ESEM imaging is employed to complement the optical visualization results and investigate the long-range ensemble coalescence events reported above, taking advantage of the enhanced depth of view and spatial resolution offered by this technique.[30,31] The sequence of images in Figure 4 shows that, upon initial cooling below saturation temperature, a layer of condensate forms at the base of the wires (Figure 4a,b) due to preferential nucleation and capillary condensation on the high-energy hydrophilic surface. We also conducted an ESEM investigation into condensation on an uncoated gold nanowire array with uniform high surface energy. In this case, the liquid sublayer continues to grow until the nanowires are completely coated with no droplets forming on the surface. A video of the process is available in the Supporting Information.

Once the hydrophilic portion is fully wetted, droplets nucleate on the hydrophobic wire tips. These droplets are initially in the Cassie state, as indicated by the fact that they are highly spherical, exhibit very high (>150°) contact angles and grow in a constant contact angle mode (Figure 4c,d). The intrinsic contact angle, θ_{young}, is roughly 108° for a fluoropolymer on a smooth surface,[32] meaning that in order to have a Cassie−Baxter contact angle of over 150° the area underneath the droplet base that contacts solid must be less than 20% of the total droplet base area. This can be determined by solving the Cassie−Baxter equation,[33] $\cos \theta_{CB} = f \times \cos \theta_{young} + (f - 1)$, where f is the fractional solid contact area underneath the droplet. This observation highlights the importance of the secondary roughness caused by the

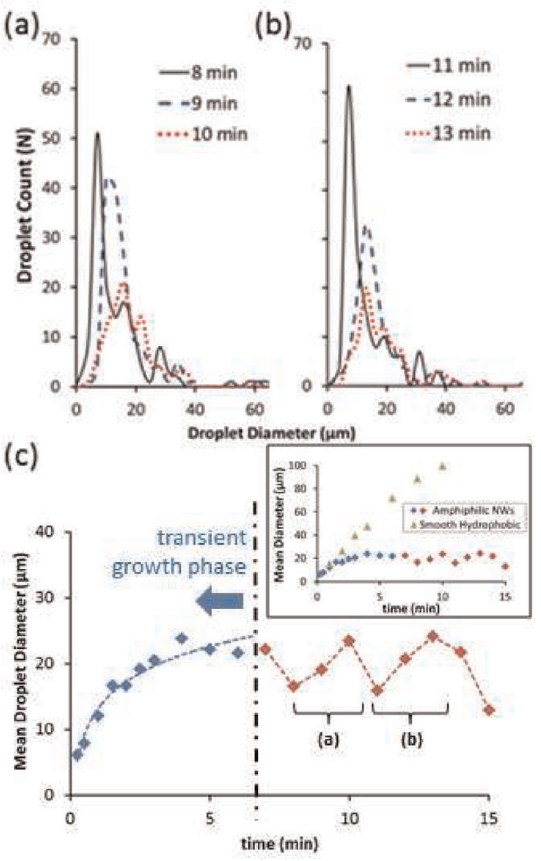

Figure 3. (a) Droplet size distributions in the 0−60 μm range at 8, 9, and 10 min past the onset of condensation on the amphiphilic nanostructured surface. (b) Size distribution 11, 12, and 13 min past condensation onset. (c) Time history of mean droplet diameter on the amphiphilic surface; time regions from the histograms in (a) and (b) are labeled to highlight periodic behavior. Inset in top right includes mean droplet diameter data on the smooth hydrophobic surface for direct comparison.

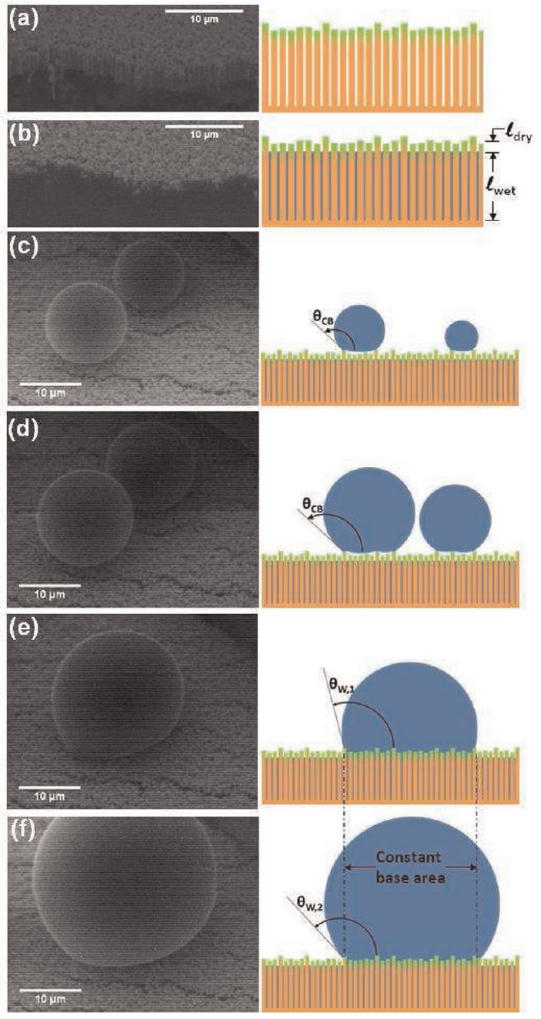

Figure 4. W ESEM images of condensation wetting stages on amphiphilic surface. (a) Dry amphiphilic surface prior to subcooling. (b) Subcooling the surface leads to nucleation at hydrophilic base of nanowires and formation of wetted sublayer. (c) Formation and (d) constant contact angle growth of Cassie droplets on hydrophobic nanowire tips. (e) Coalescence of adjacent Cassie droplets through direct contact. (e) Resulting coalesced drop is in Wenzel state, connected to wetted sublayer, as indicated by constant base area growth. See web enhanced object S4 for a video of the entire process.

difference in wire heights because, with a wire packing fraction of approximately 85%, the initial Cassie droplets must only contact a fraction of the (tallest) wires beneath it to achieve a 20% area fraction. Further, roughness features must truly be nanosized to support droplets on the order of 10 μm because a high number of wires at different heights must be present beneath this small droplet for the above-described behavior to occur.

Eventually, adjacent Cassie droplets coalesce by growing into one another, and in doing so transition to the Wenzel state wherein they are connected to the underlying fluid layer. This transition can be seen by a post-coalescence reduction in contact angle and by the fact that a coalesced droplet grows in a constant base area mode with a high degree of contact line pinning (Figure 4e,f).

The insight gained from ESEM visualization of the wetted sublayer development and initial droplet dynamics offers a more complete understanding of the phenomenon occurring in the periodic rejuvenation regime depicted in Figures 2 and 3. After undergoing at least one coalescence, droplets transition to a Wenzel state and are thus fluidically linked *via* the wetted sublayer between the hydrophilic portions of the nanowires. In the rejuvenation regime, there is an assortment of Wenzel state droplets of varying diameter within close proximity of one another. Thermodynamically, droplets on a surface will always prefer to coalesce into one larger droplet to minimize the total surface free energy; however, on a typical surface, there is no path to this lower energy state. In contrast, on the amphiphilic surface, the Laplace pressure difference between adjacent droplets with different radii of curvature supplies the driving force for coalescence and the fluidic linkage provides the pathway. A representative coalescence sequence with an illustrated schematic is highlighted in Figure 5. It is clear that the droplets do coalesce into one,

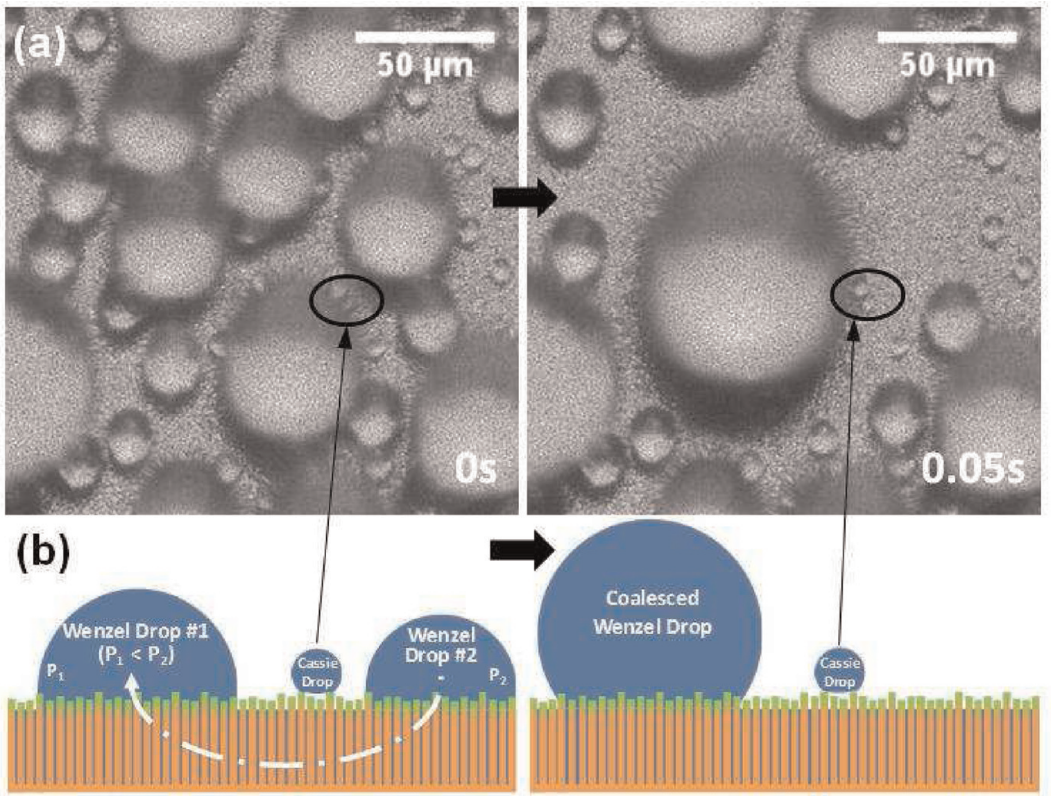

Figure 5. (a) Pre- and post-coalescence optical images of a Laplace pressure-driven multidroplet long-range coalescence event. Encircled droplets are in the Cassie state and therefore do not interact with the surrounding coalescing droplets. (b) Sketched schematic of the coalescence process.

rather than moving radially outward from the field of view, because a region of droplets fully surrounding each coalescence zone remains unaffected during the event. Furthermore, the fact that two small droplets, presumably in the Cassie state due to their small size, are unaffected by the coalescence of the surrounding droplets provides strong evidence supporting the proposed mechanism of nondirect coalescence through the wetted sublayer. If the larger Wenzel droplets were instead coalesced above the surface by a cascade of adjacent contacting droplets, these Cassie droplets would undoubtedly be swept up in the process. It is important to note, however, that both contact-based and Laplace pressure-driven coalescences can occur simultaneously, as indicated in Figure 5, by the other small Cassie droplets which are within the footprint of the final coalesced drop and therefore do participate in the coalescence.

CONCLUSION

In summary, we have reported a novel nanostructured amphiphilic surface with a vertical surface energy gradient which enables long-range collective coalescence events resulting in periodic generation of fresh nucleation sites for small droplets during dropwise condensation. ESEM visualization indicates that this regenerative behavior is achieved by Laplace pressure-driven coalescence of Wenzel droplets through the wetted sublayer, rather than requiring condensed droplets to remain stable in the Cassie state such that they can roll off the surface. High-speed visualization could provide further insight into this new phenomenon, potentially capturing the rapid transient interaction between droplets and the substrate. This type of amphiphilic surface has fabrication advantageous in that the roughness is generated in a single step, rather than requiring fabrication of microscale roughness followed by subsequent growth of nanostructures as utilized in other studies.[15−17]

The issue of removing the few large "sticky" Wenzel droplets remains and is important for practical applications of designing heat transfer equipment. However, the fact that the wetted sublayer provides a path for droplet coalescence from longer range means that the largest droplets can more rapidly collect volume and grow to a size where removal becomes practical. For example, on a vertically oriented surface, eventually, gravitational forces will become significant relative to surface forces at which point the largest droplets can slide off the surface. Alternatively, other techniques such as vibration-induced dewetting[34] may be employed to remove the largest droplets at a greater frequency. Regardless of removal mechanism, during the time in which the largest droplets grow to a size practical for removal, a heat transfer enhancement is expected in the area of the surface immediately surrounding these droplets as moderately sized

Wenzel droplets are drawn in by the Laplace pressure imbalance and fresh nucleation sites are created in their wake. With further exploration and optimization, this type of amphiphilic surface could provide an alternative mode of dropwise condensation to that of traditional superhydrophobic surfaces, thus opening new avenues for a broad range of critical moisture and thermal management applications in emerging thermally limited nanotechnologies.

METHODS

Nanowire Fabrication. To prepare the amphiphilic nanostructure, first gold nanowire arrays were fabricated by electrodeposition into 200 nm pore diameter porous alumina templates (Whatman, Anodisc). A thin gold working electrode (50 nm) was sputtered on the branched side of the alumina template. Next, gold was deposited into the template using Orotemp 24 plating solution (Technic Inc.) at a potential of −0.9 V *versus* reference electrode in a three-electrode cell (a platinum foil counter electrode and saturated calomel reference electrode were used). The length of the wires was controlled by the deposition time, typically a 1 h deposition yields 350 nm long wires. After deposition, the alumina template surrounding the wires was removed in 3 M NaOH solution and extensively rinsed with Nanopure (18.2 MΩ·cm resistivity) water. To prevent aggregation due to capillary forces during evaporation, the wire arrays were not allowed to "air dry"; instead, a freeze-drying process was used.

PECVD Hydrophobic Coating. A flowing capacitively coupled plasma-enhanced CVD system was utilized to coat the tips of the wires with a hydrophobic fluoropolymer. The PECVD system operated at a radio frequency of 13.56 MHz and power of 30 W. The monomer octafluorocyclobutane (C_4F_8) was supplied to the deposition chamber at a rate of 3 sccm, along with 50 sccm of argon gas. The chamber was held at 80 mTorr and room temperature during deposition, with the monomer inlet in the downstream position 3 in. above the substrate. Deposition time was 60 s, leading to a coating of approximately 10 nm on the tips of the nanowires. In comparison, the smooth hydrophobic surface was coated with a commercially available hydrophobic coating (Rain-X).

Scanning Electron Microscope Imaging. Condensation images are captured using an FEI Quanta 200 ESEM with pure water vapor at 5.8 Torr in the chamber. Subcooling of the surface is accomplished with a solid-state Peltier cooling device. The SEM micrographs in Figure 1 are taken with a Zeiss Ultra60 FE-SEM.

Optical Imaging with Visible Light. Video images of vapor condensation are taken normal to the test surfaces using a Phantom v12 camera with a 50× optical lens, capturing 24 frames per second and a 341.5 × 341.5 μm field of view. The surface is subcooled with a solid-state Peltier device; however, in this case, water vapor in ambient air at ~40% relative humidity is used for condensation rather than pure vapor in the ESEM.

Conflict of Interest: The authors declare no competing financial interest.

Acknowledgment. AFOSR BIONIC Center (Award No. FA9550-09-1-0162) provided financial support for this work. The authors thank A. Waite at Air Force Research Laboratory for assistance with the fluoropolymer PECVD coating process. They also acknowledge S. Naik at Georgia Institute of Technology for preparing the electrodeposited gold nanowire samples.

Supporting Information Available: Additional video. This material is available free of charge *via* the Internet at http://pubs.acs.org.

REFERENCES AND NOTES

1. Degennes, P. G. Wetting - Statics and Dynamics. *Rev. Mod. Phys.* **1985**, *57*, 827–863.
2. Kim, S. H. Fabrication of Superhydrophobic Surfaces. *J. Adhes. Sci. Technol.* **2008**, *22*, 235–250.
3. Nosonovsky, M.; Bhushan, B. Superhydrophobic Surfaces and Emerging Applications: Non-adhesion, Energy, Green Engineering. *Curr. Opin. Colloid Interface Sci.* **2009**, *14*, 270–280.
4. Crick, C. R.; Parkin, I. P. Preparation and Characterisation of Super-Hydrophobic Surfaces. *Chem.—Eur. J.* **2010**, *16*, 3568–3588.
5. Nosonovsky, M.; Bhushan, B. Biomimetic Superhydrophobic Surfaces: Multiscale Approach. *Nano Lett.* **2007**, *7*, 2633–2637.
6. Rykaczewski, K.; Scott, J. H. J. Methodology for Imaging Nano-to-Microscale Water Condensation Dynamics on Complex Nanostructures. *ACS Nano* **2011**, *5*, 5962–5968.
7. Schmidt, E.; Schurig, W.; Sellschopp, W. Condensation of Water Vapour in Film- and Drop Form. *Tech. Mech. Thermodyn.* **1930**, *1*, 53–63.
8. Rose, J. W. Dropwise Condensation Theory and Experiment: A Review. *Proc. Inst. Mech. Eng., Part A* **2002**, *216*, 115–128.
9. Carey, V. P. *Liquid-Vapor Phase-Change Phenomena: An Introduction to the Thermophysics of Vaporization and Condensation Processes in Heat Transfer Equipment*; Hemisphere Pub. Corp.: Washington, DC, 1992.
10. Graham, C.; Griffith, P. Drop Size Distributions and Heat-Transfer in Dropwise Condensation. *Int. J. Heat Mass Transfer* **1973**, *16*, 337–346.
11. Rose, J. W.; Glicksman, L. R. Dropwise Condensation - Distribution of Drop Sizes. *Int. J. Heat Mass Transfer* **1973**, *16*, 411–425.
12. Dorrer, C.; Ruhe, J. Some Thoughts on Superhydrophobic Wetting. *Soft Matter* **2009**, *5*, 51–61.
13. Quere, D. Non-sticking Drops. *Rep. Prog. Phys.* **2005**, *68*, 2495–2532.
14. Lau, K. K. S.; Bico, J.; Teo, K. B. K.; Chhowalla, M.; Amaratunga, G. A. J.; Milne, W. I.; McKinley, G. H.; Gleason, K. K. Superhydrophobic Carbon Nanotube Forests. *Nano Lett.* **2003**, *3*, 1701–1705.
15. Chen, C. H.; Cai, Q. J.; Tsai, C. L.; Chen, C. L.; Xiong, G. Y.; Yu, Y.; Ren, Z. F. Dropwise Condensation on Superhydrophobic Surfaces with Two-Tier Roughness. *Appl. Phys. Lett.* **2007**, *90*, 173108-1–173108-3.
16. Boreyko, J. B.; Chen, C. H. Self-Propelled Dropwise Condensate on Superhydrophobic Surfaces. *Phys. Rev. Lett.* **2009**, *103*, 184501-1–184501-4.
17. Chen, X.; Wu, J.; Ma, R.; Hua, M.; Koratkar, N.; Yao, S.; Wang, Z. Nanograssed Micropyramidal Architectures for Continuous Dropwise Condensation. *Adv. Funct. Mater.* **2011**, *21*, 4617–4623.
18. Varanasi, K. K.; Hsu, M.; Bhate, N.; Yang, W. S.; Deng, T. Spatial Control in the Heterogeneous Nucleation of Water. *Appl. Phys. Lett.* **2009**, *95*, 094101-1–094101-3.
19. Dietz, C.; Rykaczewski, K.; Fedorov, A. G.; Joshi, Y. Visualization of Droplet Departure on a Superhydrophobic Surface and Implications to Heat Transfer Enhancement during Dropwise Condensation. *Appl. Phys. Lett.* **2010**, *97*, 033104-1–033104-3.
20. Patankar, N. A. Supernucleating Surfaces for Nucleate Boiling and Dropwise Condensation Heat Transfer. *Soft Matter* **2010**, *6*, 1613–1620.
21. Cheng, Y. T.; Rodak, D. E. Is the Lotus Leaf Superhydrophobic? *Appl. Phys. Lett.* **2005**, *86*, 144101-1–144101-4.
22. Narhe, R. D.; Beysens, D. A. Nucleation and Growth on a Superhydrophobic Grooved Surface. *Phys. Rev. Lett.* **2004**, *93*, 076103-1–076103-4.
23. Wier, K. A.; McCarthy, T. J. Condensation on Ultrahydrophobic Surfaces and Its Effect on Droplet Mobility:

Ultrahydrophobic Surfaces Are Not Always Water Repellant. *Langmuir* **2006**, *22*, 2433–2436.
24. Lafuma, A.; Quere, D. Superhydrophobic States. *Nat. Mater.* **2003**, *2*, 457–460.
25. Patankar, N. A. Transition between Superhydrophobic States on Rough Surfaces. *Langmuir* **2004**, *20*, 7097–7102.
26. Marmur, A. Wetting on Hydrophobic Rough Surfaces: To Be Heterogeneous or Not To Be? *Langmuir* **2003**, *19*, 8343–8348.
27. Anderson, K. D.; Slocik, J. M.; McConney, M. E.; Enlow, J. O.; Jakubiak, R.; Bunning, T. J.; Naik, R. R.; Tsukruk, V. V. Facile Plasma-Enhanced Deposition of Ultrathin Crosslinked Amino Acid Films for Conformal Biometallization. *Small* **2009**, *5*, 741–749.
28. Daniel, S.; Chaudhury, M. K.; Chen, J. C. Fast Drop Movements Resulting from the Phase Change on a Gradient Surface. *Science* **2001**, *291*, 633–636.
29. Ristenpart, W. D.; McCalla, P. M.; Roy, R. V.; Stone, H. A. Coalescence of Spreading Droplets on a Wettable Substrate. *Phys. Rev. Lett.* **2006**, *97*, 064501-1–064501-4.
30. Jung, Y. C.; Bhushan, B. Wetting Behaviour during Evaporation and Condensation of Water Microdroplets on Superhydrophobic Patterned Surfaces. *J. Microsc.* **2008**, *229*, 127–140.
31. Rykaczewski, K.; Scott, J. H. J.; Fedorov, A. G. Electron Beam Heating Effects during Environmental Scanning Electron Microscopy Imaging of Water Condensation on Superhydrophobic Surfaces. *Appl. Phys. Lett.* **2011**, *98*, 093106-1–093106-3.
32. Fox, H. W.; Zisman, W. A. The Spreading of Liquids on Low Energy Surfaces. I. Polytetrafluoroethylene. *J. Colloid Sci.* **1950**, *5*, 514–531.
33. Cassie, A. B. D.; Baxter, S. Wettability of Porous Surfaces. *Trans. Faraday Soc.* **1944**, *40*, 0546–0550.
34. Boreyko, J. B.; Chen, C. H. Restoring Superhydrophobicity of Lotus Leaves with Vibration-Induced Dewetting. *Phys. Rev. Lett.* **2009**, *103*, 174502-1–174502-4.